CHAPTER III
DEVELOPMENT OF POLYCAPROLACTONE POROUS SCAFFOLDS BY COMBINING SOLVENT CASTING, PARTICULATE LEACHING, AND POLYMER LEACHING TECHNIQUES FOR BONE TISSUE ENGINEERING

3.1 Abstract

Sodium chloride and polyethylene glycol (PEG) were used as water-soluble porogens for the formation of porous polycaprolactone (PCL) scaffolds. The main purpose was to prepare and evaluate in vitro efficacy of highly interconnected, three-dimensional, porous polymeric scaffolds, as obtained from the combined particulate and polymer leaching techniques. Microscopic analysis confirmed the high interconnectivity of the pores and relatively uniform pore size of 378–435 µm. The PCL scaffolds were further characterized for their density and pore characteristics, water absorption and flow behaviors, and mechanical properties and the potential for their use as bone scaffolding materials was evaluated in vitro using mouse calvaria-derived preosteoblastic cells (MC3T3-E1). Evidently, the use of PEG as the secondary porogen not only improved the interconnectivity of the pore structures but also resulted in the PCL scaffolds that exhibited much better support for the proliferation and differentiation of the cultured bone cells.

(**Key Words**: polycaprolactone, bone scaffolds, solvent casting/particulate leaching method, polymer leaching method, dual leaching method)

3.2 Introduction

A variety of natural and synthetic polymers have been utilized to fabricate tissue engineering scaffolds. These materials must be inherently biocompatible, biodegradable, and highly cell adhesive. Additionally, the polymers must be porous and mechanically stable and exhibit a three-dimensional (3D) structure that can be obtained via a facile manufacturing processes. Aliphatic polyesters, such as

polycaprolactone (PCL), polylactic acid (PLA), polyglycolic acid (PGA), and related copolymers, are the most extensively used in biodegradable scaffolds because of these polymers' excellent biocompatibility, biodegradability, bioresorbability, and mechanical strength. These materials have been approved by the Food and Drug Administration (FDA) and are easily processed into various structures with 3D matrices.[1, 2]

PCL is a semi-crystalline polyester that is degraded by the hydrolysis of its ester linkages under physiological conditions, such as in the human body. In particular, PCL is useful for the preparation of long-term implants due to its markedly slow degradation rate. This polymer has received FDA approval and is already used in drug delivery devices, sutures, and adhesion barriers. Additionally, due to its excellent biocompatibility, mechanical strength, lack of toxicity, and low cost, PCL is one of the biodegradable polyesters that has attracted the most attention in bone tissue engineering.[2-3]

The potential use of porous biodegradable scaffolds as 3D templates to encourage initial cell attachment and subsequent tissue formation has been studied both in vitro and in vivo. Various tissues, such as cartilage, bone, heart, nerve, muscle, bladder, and liver tissues, have been produced using such scaffolds. In these applications, the scaffolds should be highly porous to allow cell seeding and facilitate invasion by blood vessels, which supply nutrients to and remove waste from the transplanted cells. The scaffold architecture should permit cell intrusion, nutrient and waste product permeation, and new capillary network formation. A scaffold's porosity is another fundamental characteristic that is necessary to provide for cell migration and tissue vascularization. Furthermore, cellular interactions increase as the available surface area is expanded. Generally, the biological activity of a scaffold is determined by the construct's ligand density, which is determined by the scaffold's composition and porous fraction, which is the total surface of the structure that is exposed to the cells. Highly customized surface areas can encourage cell attachment and anchorage, and a high pore-volume fraction enables cell growth and migration and the effective transport of fluids and nutrients. In sum, to best mimic a tissue, scaffolds should be designed to be highly porous and to exhibit a high surface area, fully interconnected geometry, structural strength, and a specific 3D shape.[4-6]

Various techniques have been reported for the preparation of porous polymeric scaffolds. A wide range of techniques commonly used in tissue engineering generate constructs with random structures, unpredictable pore sizes, and reduced pore interconnectivity. Any variation in porosity within the 3D structure cannot be controlled, and the mechanical strength, structural stability, and reproducibility of these scaffolds are generally low. Among these techniques, solvent casting, freeze drying, phase inversion, fiber bonding, melt-based technologies, and high pressure-based methods are the most commonly used.[7] Porous polymers can be prepared by embedding soluble ingredients, known as porogens, into the polymer, which form pores in the polymer matrix upon removal. In modern tissue engineering, solvent casting is often used in combination with other common methods to produce a porous 3D structure. For example, solvent casting combined with particulate leaching has been used to successfully fabricate 3D scaffolds. The porogens typically used in the field are sodium chloride, ammonium bicarbonate, and glucose with different crystal sizes.[8-12]

The porogen leaching technique for solvent-cast scaffolds involves pouring a polymer solution (e.g., PLA in chloroform) onto a bed of porogens, such as salt particles, paraffin microspheres or emulsion particles of a defined size. The solvent is evaporated, resulting in the solidification of the polymer around the porogen particles. The entrapped porogen is then leached out of the scaffold using numerous rinses with distilled water (in the case of NaCl) or an organic solvent (in the case of paraffin), thereby creating a defined pore structure. This leaching strategy has been applied to the creation of porous scaffolds for the growth of endothelial cells.[13] Such a construct's biochemical properties and architecture should support cell attachment, migration, growth, and ultimately, tissue maturation.[14] In particular, the achievement of an open, interconnected pore system within a 3D structure is critical for ensuring proper nutrient and waste transport, tissue ingrowth, vascularization, and eventually, the integration of the construct within the host.[15]

Blended polymers play an important role in the development of microporous controlled-delivery systems. Typically, there are two types of polymers present in blended membranes: one polymer remains for the end use, whereas the other polymer, used only to produce pores in the membranes, is removed. Due to its

specific properties, such as water solubility, polyethylene glycol (PEG) is frequently used as a polymeric additive to generate membranes and is a common coating material in biomaterial applications. The pores can be created in scaffolds by leaching out the water-soluble PEG using the solvent casting and polymer leaching methods.[15-18] The preparation method proposed here combines solvent casting and salt particulate leaching with polymer leaching, with the purpose of improving the pore interconnectivity of 3D polymeric scaffolds.

3.3 Experimental

3.3.1 Materials

PCL (80,000 gmol^{-1}) was purchased from Sigma-Aldrich (St.Louis, USA), and PEG (MW = 200, 600, and 1,000 gmol^{-1}) was purchased from Merck (Germany). Chloroform (Labscan Asia, Thailand) was used as a solvent for these polyesters, whereas sodium chloride (Ajax Finechem, Australia) was used as a porogen. All of the other chemicals were of analytical reagent grade and were used without further purification.

3.3.2 Preparation of PCL Scaffolds

The solvent casting, polymer leaching, and salt particulate leaching techniques were used to prepare the scaffolds. Briefly, a polymer solution was prepared by mixing a PCL pellet with PEG and chloroform at a concentration of 28% (w/v). The solution was then stirred at room temperature for 2-3 h. Next, NaCl particles ranging in diameter from 400-500 μm (polymer/NaCl = 1/30 (w/w)) were added. The mixture was packed into Petri dishes, creating cylindrical molds that were 1.2 mm in diameter and 0.8 mm in thickness. These molds were placed in a ventilation hood overnight to allow solvent evaporation. After evaporation, to leach out the PEG and salt particles, the constructs were immersed in deionized (DI) water for 48 h, with repeated changes of the DI water every 8 h. The scaffolds were then air-dried for 24 h and vacuum-dried overnight. The resultant salt-PEG leached PCL scaffolds exhibited highly interconnected porous networks. Prior to casting, the

viscosity of each of the PCL and PCL-PEG blend solutions was characterized at room temperature (i.e., 25 ± 1°C) using a Brookfield DV-III programmable viscometer.

3.3.3 Characterization of PCL Scaffolds

Microstructural Observation

The pore morphology, size, distribution, and interconnectivity of the porous scaffolds were observed using a JEOL JSM-5200 scanning electron microscope, Olympus SZH10 stereomicroscope, and Carl Zeiss Mirax desk visual slide microscope. One cylindrical scaffold was randomly selected from each group, cut with a razor blade in the middle and mounted onto a stub. These cross sections were coated with a thin film of gold using a JEOL JFC-1100E sputtering device for 5 min prior to observation by scanning electron microscopy (SEM).

Porosity, Pore Volume, and Pore Size

The porosity and pore volume of the scaffolds were determined gravimetrically, according to the following equations:

$$Porosity\,(\%) = \left(1 - \frac{\rho\ scaffold}{\rho\ polymer}\right) x\ 100$$

$$Pore\ volume\,(\%) = \left(\frac{1}{\rho\ scaffold} - \frac{1}{\rho\ polymer}\right) x\ 100$$

where $\rho_{polymer}$ is the density of the polymer from which the scaffolds were fabricated, and $\rho_{scaffold}$ is the apparent density of the scaffolds, determined using a Sartorius YDK01 density measurement kit. Here, ρ_{PCL} was considered to be 1.145 gcm^{-1}. Five specimens were assessed for both porosity and pore volume, and an average value was calculated for each property. In contrast, the pore size of each scaffold was directly measured from the SEM images using a SemAfore Digital slow-scan image-recording system (version 5.0 software). At least 30 pores for each of the cross and longitudinal sections (i.e., at least 60 pores in total) were analyzed, and average values were calculated for all of the scaffolds investigated.

Water Absorption Capacity

The scaffold specimens were cut from the molds, which were created by casting in Petri dishes with a circular shape measuring 15 mm in diameter and 3 mm in height. The constructs were first dried, weighed, and individually immersed in 10 ml of 10 mM phosphate-buffered saline (PBS; pH 7.4) at room temperature. At a specified point in time, the specimens were removed from the solution, carefully placed on glass for 5 sec to remove any excess water, and weighed immediately. The amount of water retained in each scaffold was determined according to the following equation:

$$Water\ absorption\,(\%) = \frac{(Ww - Wd)}{Ww} \times 100$$

where W_d and W_w are the weights of the specimen before and after submersion in the medium, respectively. This experiment was conducted in pentuplicate, and measurements were performed at different time points within a period of 14 d.

Water Permeability

To obtain information regarding pore interconnectivity, the flow resistance of the constructs was evaluated by sealing the scaffolds between two rubber rings at the bottom of a measuring tube filled with 10 cm of water. To keep the water level as even as possible during flow, the tube was in contact with a large-diameter reservoir. Before each test, the sample was preconditioned in water for 24 h. The flow resistance of each scaffold was then evaluated as the time required for 10 ml of water to flow through the pores.

Compressive Modulus

The compressive modulus of each scaffold was determined using a universal testing machine (Lloyd LRX, UK) and a load cell of 500 N in a dry state at room temperature. The load was vertically compressed at a crosshead speed of 3 mm/min until the scaffolds were reduced to approximately 70% of the original thickness. The initial compressive modulus was then determined from the slope of the linear portion of the stress-strain curve at a compressive strain of 20%.

3.3.4 Biological Characterization of PCL Scaffolds

Cell Culture and Seeding

Mouse fibroblasts (L929) and mouse calvaria-derived pre-osteoblastic cells (MC3T3-E1) were used as reference cell lines. The L929 cells were cultured as a monolayer in Dulbecco's modified Eagle's medium (DMEM; Sigma-Aldrich, USA) supplemented with 10% fetal bovine serum (FBS; BIOCHROM AG); 1% L-glutamine (Invitrogen); and 1% antibiotic and antimycotic formulation, containing penicillin G sodium, streptomycin sulfate, and amphotericin B (Invitrogen, USA). The MC3T3-E1 cells were cultured in Minimum Essential Medium (MEM; Hyclone, USA) with Earle's Balanced Salts and supplemented with 10% FBS (BIOCHROM AG, Germany), 1% L-glutamine (Invitrogen, USA), and 1% antibiotic and antimycotic formulation, as described above. The media were replaced every 2 days, and the cultures were maintained at 37°C in a humidified atmosphere containing 5% CO_2.

Each scaffold was cut into circular discs of approximately 15 mm in diameter, which were placed into the wells of a 24-well tissue-culture polystyrene (TCPS) plate. The discs were then sterilized in 70% ethanol for 30 min, washed with autoclaved DI water and PBS, and immersed in MEM overnight. To ensure complete contact between the scaffolds and the wells, each construct was pressed with a metal ring of approximately 12 mm in diameter.

The cultured MC3T3-E1 cells were detached using 0.25% trypsin containing 1 mM EDTA (Invitrogen, USA) and counted with a hemacytometer (Hausser Scientific, USA). The cells were then seeded on the scaffolds at a density of approximately 40,000 cells/well for the attachment and proliferation studies. Seeded, empty wells of a TCPS plate were used as a control. For the indirect cytotoxicity, alkaline phosphatase activity, and mineralization evaluations, the MC3T3-E1 cells were seeded at a density of approximately 40,000 cells/well on the scaffolds and empty wells of a TCPS plate. The culture was maintained in an incubator at 37°C with a humidified atmosphere containing 5% CO_2.

Cytotoxicity Evaluation

Two cell types were used for the cytotoxicity evaluation: 1) mouse calvaria-derived pre-osteoblastic cells (MC3T3-E1) and 2) mouse fibroblasts (L929). In particular, an indirect cytotoxicity test was conducted on TCPS wells and on salt leached PCL, salt-PEG 200 leached PCL, salt-PEG 600 leached PCL, and salt-PEG 1000 leached PCL scaffolds. First, the extraction media were prepared by immersing the samples, which were approximately 15 mm in diameter, in serum-free medium (SFM) containing DMEM (for the L929 cells) or MEM (for the MC3T3-E1 cells), supplemented with 1% L-glutamine, 1% lactalbumin, and 1% antibiotic and antimycotic formulation, for 1, 3, or 7 days. Each of these extraction media was then used to evaluate the cytotoxicity of the scaffolds. Either the L929 cells or the MC3T3-E1 cells were cultured in the wells of a 24-well culture plate containing 10% FBS-supplemented DMEM or MEM, respectively, for 16 h to allow cell attachment to the plate. Next, the cells were starved in SFM for 24 h, after which the medium was replaced with extraction medium. After an additional 24 h of cell culture, a 3-(4,5-dimethylthiazol-2-yl)-2,5-diphenyl-tetrazolium bromide (MTT) assay was performed to quantify the number of viable cells. These experiments were conducted in triplicate.

MTT Assay

The MTT assay is based on the reduction of yellow tetrazolium salt to purple formazan crystals by dehydrogenases secreted by the mitochondria of metabolically active cells. The amount of purple formazan crystals formed is proportional to the number of viable cells. In the current study, the culture medium was first aspirated and replaced with 400 ml/well of MTT solution at 0.5 mg/ml in a 24-well culture plate. Second, each plate was incubated for 30 min at 37°C. The MTT solution was then aspirated, and 1 ml/well of dimethyl sulfoxide (DMSO) containing 125 μl/well of glycine buffer (pH 10) was added to dissolve the formazan crystals. Finally, after 5 min of rotary agitation, the absorbance of the DMSO solution at 540 nm was measured using a Thermo Spectronic Genesis10 UV/Visible spectrophotometer.

o

Cell Attachment and Proliferation

Cell behaviors, such as adhesion and proliferation, represent the initial phase of cell-scaffold communication, which subsequently affects cell differentiation and mineralization. In the attachment study, the MC3T3-E1 cells were allowed to adhere to the TCPS, salt leached PCL, salt-PEG 200 leached PCL, salt-PEG 600 leached PCL, and salt-PEG 1000 leached PCL for 2, 4 or 6 h. Each sample was then rinsed with PBS to remove unattached cells prior to morphological assessment of the adherent cells by SEM. In the proliferation study, the viability of the cells on the scaffolds was determined after 1, 2, or 3 days of cell culture by DNA quantification. These experiments were performed in triplicate.

DNA Quantification

The amount of DNA, signifying the number of proliferating cells that had been cultured on each of the scaffolds for 1, 2, or 3 days, was quantified using a DNA Quantification Kit (Sigma-Aldrich, USA). Briefly, the cultured cells were thoroughly washed twice with 400 μL of PBS and then lysed with 400 μL of a cell lysis buffer. The resultant suspension was centrifuged for 10 min to precipitate cell debris, and 20 μL of the supernatant was mixed with 2 ml of 0.1 μg/ml Bisbenzimide H 33258 solution in 10X Fluorescent Assay Buffer. The fluorescent emission intensity of this solution was measured at 460 nm after excitation at 360 nm using a microplate reader.

Morphological Observation of Cultured Cells

After removal of the culture medium, the cell-seeded scaffolds were rinsed twice with PBS and fixed in 3% glutaraldehyde solution, which was diluted from 50% glutaraldehyde solution (Sigma, USA) with PBS, at 500 μl/well. After 30 min, the wells were again rinsed with PBS. Following cell fixation, the specimens were dehydrated in ethanol solutions of varying concentrations (i.e., 30, 50, 70, 90, and 100%) for approximately 2 min at each concentration and dried in 100% hexamethyldisilazane (HMDS; Sigma, USA) for 5 min. The scaffolds were allowed to air-dry after the removal of the HMDS. The completely dry specimens were mounted on SEM stubs, coated with gold, and observed using a JEOL JSM-5200 scanning electron microscope.

Production of Alkaline Phosphatase (ALP) by Cultured Cells

The ALP activity of the MC3T3-E1 cells was measured using Alkaline Phosphate Yellow Liquid. In this reaction, ALP catalyzes the hydrolysis of the colorless organic phosphate-ester substrate *p*-nitrophenyl phosphate (pNPP) to a yellow product, p-nitrophenol, and a phosphate. In the present study, the MC3T3-E1 cells were cultured on scaffold specimens for 3, 5, or 7 days to observe the production of ALP. The specimens were then rinsed twice with PBS after the removal of the culture medium. Alkaline lysis buffer (10 mM Tris-HCl, 2 mM $MgCl_2$, and 0.1% Triton X-100, pH 10 was added at 200 µl/well, and the samples were scraped and frozen at -20°C for at least 30 min prior to the next step. An aqueous solution of 2 mg/ml pNPP (Zymed Laboratories, USA) mixed with 0.1 M amino propanol (10 µl/well) in 2 mM $MgCl_2$ (100 µl/well) at a pH 10.5 was prepared and added to the specimens (110 µl/well), followed by incubation at 37°C for 15 min. The reaction was stopped by adding 900 µl/well of 50 mM NaOH, and the extracted solution was transferred to a cuvette and placed in the UV-visible spectrophotometer, from which the absorbance at 410 nm was measured. The amount of ALP was then calculated using a standard curve. To determine the ALP activity, the amount of ALP was normalized to the total amount of protein synthesized.

In the protein assay, the samples were treated in the same manner as in the ALP assay up to the point at which the specimens were frozen. After freezing, bicinchoninic acid (BCA; Pierce Biotechnology, USA) solution was added to the scaffolds, which were then incubated at 37°C for 15 min. The absorbance of the medium was measured at 562 nm using the UV-visible spectrophotometer, and the total amount of protein was calculated using a standard curve.

Mineralization Analysis

Alizarin Red S dye binds selectively to calcium salts and is widely used for mineral staining (i.e., the staining product is an Alizarin Red S calcium chelating product). The isolated MC3T3-E1 cells were plated on 24-well plates at 40,000 cells/well and maintained in culture medium. After 24 h, the cultures were treated with medium supplemented with 50 µg/ml ascorbic acid (Sigma, USA), 5 mM β-glycerophosphate (Sigma, USA), and 0.2 µg/ml dexamethasone (Sigma,

USA), which was replaced every 2 days. After 14 days of treatment, the cells were washed with PBS, fixed in ice-cold absolute methanol for 10 min, and stained with 1% Alizarin Red S in DI water (Sigma, USA) at pH 4.2 for 2-3 min. After removing the alizarin red S solution, the cells were rinsed with DI water and dried at room temperature. The images of each culture were captured, and the stain was extracted using 10% cetylpyridinium chloride (Sigma, USA) in 10 mM sodium phosphate for 1 h. The absorbance of the collected dye was read at 570 nm using a UV-visible spectrophotometer (Thermo Spectronics Genesis10).

3.3.5 Statistical Analysis

All of the values were expressed as the mean ± standard deviation. Statistical analyses of the different data groups were performed by one-way analysis of variance (ANOVA), along with the least-significant difference (LSD) test, using SPSS software version 11.5. Values with $p < 0.05$ were considered statistically significant.

3.4 Results

3.4.1 Preparation of PCL Scaffolds

Table 3.1 shows the viscosities of the PCL and PEG-PCL blend solutions in chloroform. The viscosity of the PCL solution was 1064 ± 15 cP on average, whereas the viscosity of the PEG-PCL blend solutions ranged from 989-1106 cP on average.

Table 3.1 Viscosities of the PCL and the PCL-PEG blend solutions

	PCL solution	PCL-PEG 200 blend solution	PCL-PEG 600 blend solution	PCL-PEG 1000 blend solution
Viscosity (cP)	1064 ± 15	989 ± 25	1055 ± 35	1106 ± 27

3.4.2 Characterization of PCL scaffolds

Microstructural observation

Figure 3.1 shows the stereomicroscope images of the porous scaffolds formed using PCL, different types of PEG, and NaCl in chloroform, following NaCl and PEG leaching in DI water. Figures 3.2 and 3.3 display the visual slide microscope images of these porous PCL scaffolds, and Figures 3.4 and 3.5 include SEM micrographs of the microporous scaffolds formed by PCL/PEG blends including various types of PEG (MW = 200, 600, and 1,000 g/mol). Highly interconnected pores were formed in the scaffolds after the PEG was leached out in an aqueous medium, corresponding to the transparent regions shown in the stereomicroscope and visual slide microscope images. The pores in the scaffolds prepared by leaching the PEG were larger than the pores formed without PEG leaching, and these larger channels were more interconnected and evenly distributed throughout the scaffold. Well-defined, interconnected pores, detected by optical microscopy and SEM analysis of the PCL scaffolds, resulted from the use of the salt and PEG leaching techniques. However, an irregular pore geometry was obtained for both the salt leached and salt-PEG leached scaffolds, with pore dimensions ranging between 378 and 435 μm, on average (n ≥ 30).
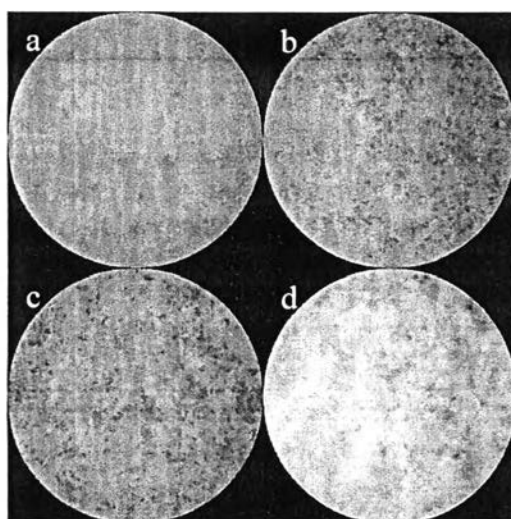
Figure 3.1 Stereomicroscope images of the (a) salt leached, (b) salt-PEG 200 leached, (c) salt-PEG 600 leached, and (d) salt-PEG 1000 leached PCL scaffolds.
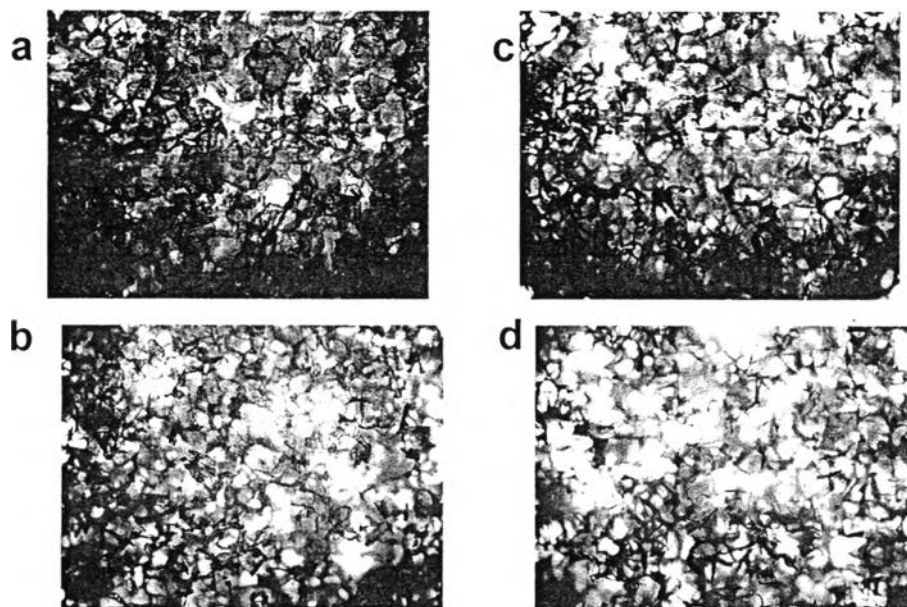
Figure 3.2 Visual slide microscope images at 5x magnification of the (a) salt leached, (b) salt-PEG 200 leached, (c) salt-PEG 600 leached, and (d) salt-PEG 1000 leached PCL scaffolds.
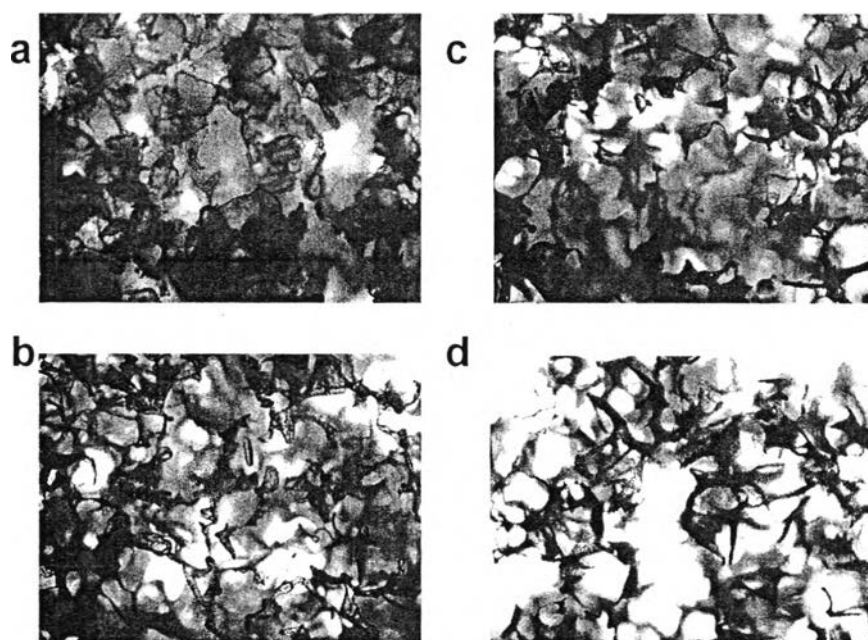
Figure 3.3 Visual slide microscope images at 10x magnification of the (a) salt leached, (b) salt-PEG 200 leached, (c) salt-PEG 600 leached, and (d) salt-PEG 1000 leached PCL scaffolds.
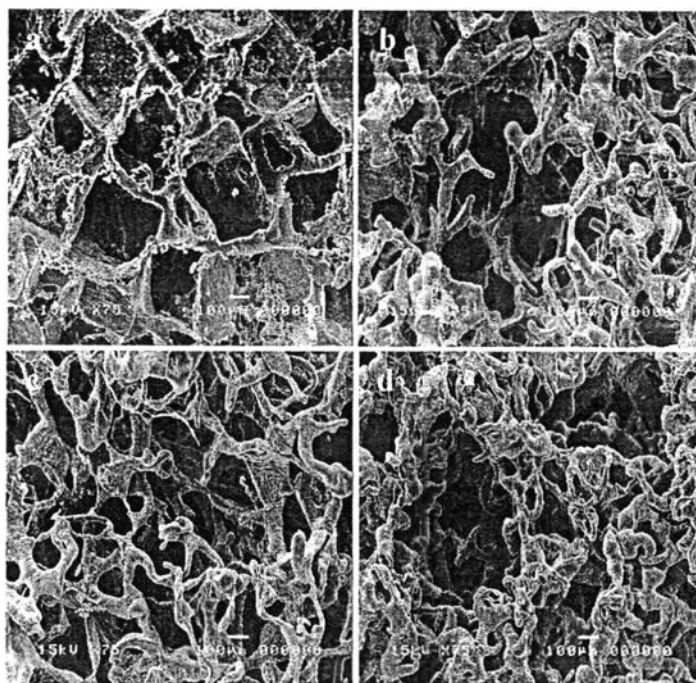
Figure 3.4 SEM images at 75x magnification illustrating the microstructures of the (a) salt leached, (b) salt-PEG 200 leached, (c) salt-PEG 600 leached, and (d) salt-PEG 1000 leached PCL scaffolds.
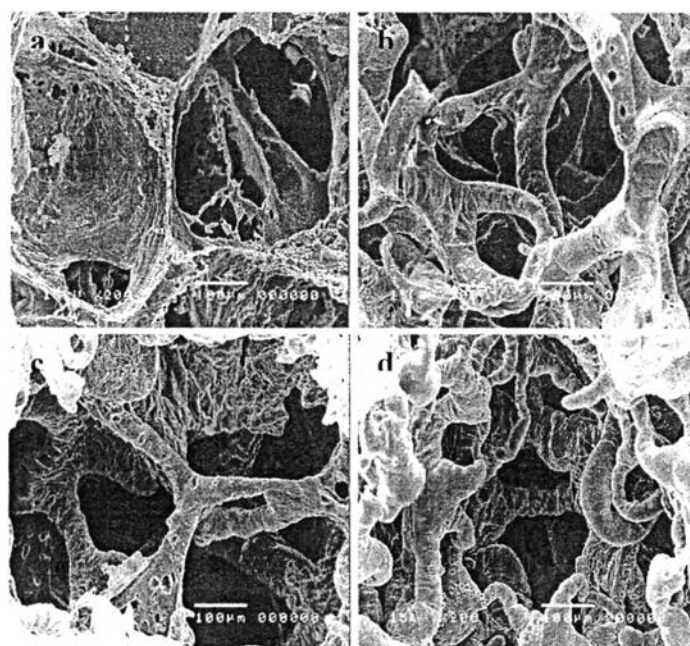
Figure 3.5 SEM images at 200x magnification illustrating the microstructures of the (a) salt leached, (b) salt-PEG 200 leached, (c) salt-PEG 600 leached, and (d) salt-PEG 1000 leached PCL scaffolds.

Porosity, Pore Volume, and Pore Size

As shown in Table 3.2, the scaffolds' porosity was reversely related to the density. The porosity of the salt leached PCL scaffolds was 91.6% on average, whereas the porosity of the salt-PEG leached PCL scaffolds ranged from 91.2-92.6% on average (n = 5). The density of these constructs was between 0.096 and 0.101 g/cm^3. In particular, the porosity increased from approximately 91.6% for the salt leached scaffolds to approximately 91.8% for the salt-PEG 600 leached scaffolds and 92.6% for the salt-PEG 1000 leached scaffolds. Similarly, the pore volume increased from 9.6 cm^{3}g^{-1} for the salt leached scaffolds to 9.9 cm^{3}g^{-1} and 10.9 cm^{3}g^{-1} for the salt-PEG 600 leached and salt-PEG 1000 leached PCL scaffolds, respectively. As expected, the pore volume increased with increasing porosity.

Table 3.2 Density, percentage of porosity, pore volume, and pore size of the scaffolds. The superscripts a, b, c, and d i n d i c a t e significant differences, with $p <$ 0.05, for an individual feature, as determined by one-way ANOVA with Tukey's honestly significant difference (HSD) test (n = 5 for porosity and pore volume, and n = 30 for pore size)

Scaffolds	Density* (g/cm^3)	Porosity* (%)	Pore volume* (cm^3/g)	Pore size* (μm)	Compressive modulus (kPa)
Salt leached PCL scaffold	0.0961	91.60 ± 0.52	9.56 ± 0.61	421.27 ± 34.18[b]	88.46 ± 15.38
Salt-PEG 200 leached PCL scaffold	0.1012[d]	91.16 ± 1.41[d]	9.18 ± 1.55	378.77 ± 82.13[a, c, d]	28.85 ± 6.80
Salt-PEG 600 leached PCL scaffold	0.0935	91.83 ± 0.61	9.87 ± 0.82	423.07 ± 40.83[b]	42.95 ± 7.85
Salt-PEG 1000 leached PCL scaffold	0.0852[b]	92.56 ± 0.43[b]	10.90 ± 0.68	434.13 ± 36.74[b]	49.98 ± 8.04

Water Absorption Capacity

Figure 3.6 illustrates the water absorption capacities of the salt leached, salt-PEG 200 leached, salt-PEG 600 leached, and salt-PEG 1000 leached PCL scaffolds in 0.1 M PBS at room temperature over 7 days. All of the salt-PEG leached PCL scaffolds exhibited similar water absorption, with the absorption rate increasing rapidly in the first 30 min and stabilizing after 24 h. In contrast, the salt leached PCL scaffolds had a different water absorption profile, with the absorption rate increasing slightly over the first 24 h and then stabilizing. Moreover, the water absorption capabilities of the PCL scaffolds were compared at 24 h, and it was found that the salt leached PCL scaffolds exhibited the lowest level of water absorption in comparison with the other constructs.

Water Absorption Capacity of Scaffolds

(a)
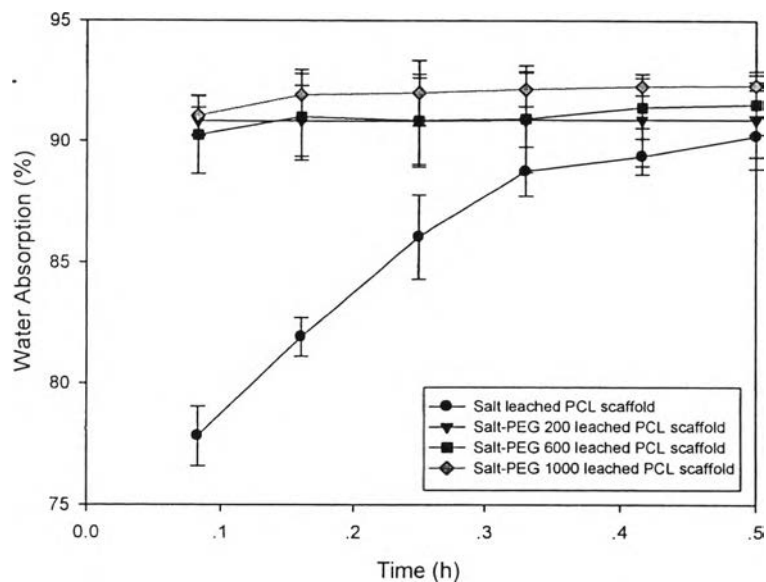
Water Absorption Capacity of Scaffolds
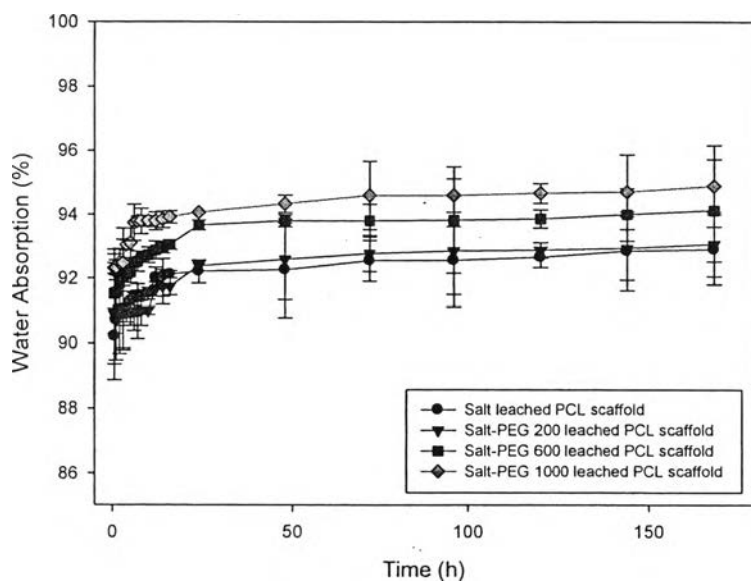
(b)

Figure 3.6 (a)Water absorption capacity of the salt leached and salt-PEG leached PCL scaffolds in 0.1 M PBS at room temperature over 30 min. (b)Water absorption capacity of the salt leached and salt-PEG leached PCL scaffolds in 0.1 M PBS at room temperature over 7 days.

Water Permeability

Figure 3.7 depicts the flow resistance for the salt leached, salt-PEG 200 leached, salt-PEG 600 leached, and salt-PEG 1000 leached PCL scaffolds. The flow resistance ranged from 14.2-21.6 sec/10 ml (for a distance of 15-50 cm) for the salt leached PCL, from 11.1-15 sec/10 ml (for a distance of 15-50 cm) for the salt-PEG 200 leached PCL, from 11.7-13.5 sec/10 ml (for a distance of 15-50 cm) for the salt-PEG 600 leached PCL, and from 10.2-13.2 sec/10 ml (for a distance of 15-50 cm) for the salt-PEG 1000 leached PCL.
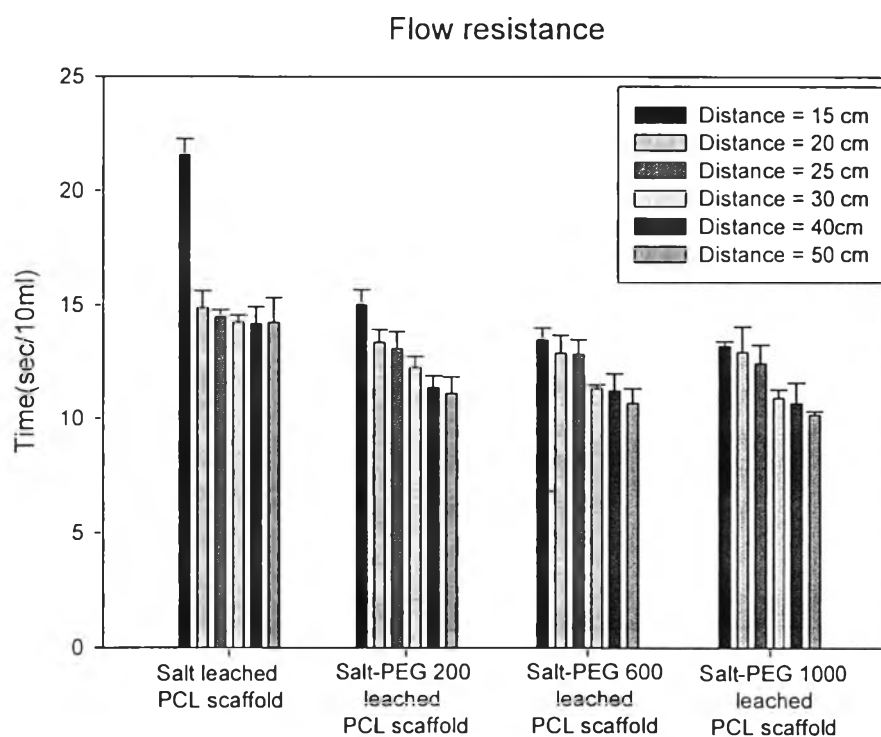
Figure 3.7 Flow resistance of the salt leached and salt-PEG leached PCL scaffolds.

Compressive Modulus

The increased porosity of the scaffolds resulted in decreased compressive properties. More specifically, the compressive modulus declined from approximately 88 kPa for the salt leached scaffold to 28, 42, and 49 kPa for the salt-PEG 200 leached, salt-PEG 600 leached, and salt-PEG 1000 leached PCL constructs, respectively. The compressive modulus of the scaffolds was thus found to fit the following decreasing trend: salt leached > salt-PEG 1000 leached > salt-PEG 600 leached > salt-PEG 200 leached PCL scaffolds.

Table 3.2 Density, percentage of porosity, pore volume, and pore size of the scaffolds. The superscripts a, b, c, and d indicate significant differences, with $p < 0.05$, for an individual feature, as determined by one-way ANOVA with Tukey's honestly significant difference (HSD) test (n = 5 for porosity and pore volume, and n = 30 for pore size)

Scaffolds	Density* (g/cm^3)	Porosity* (%)	Pore volume* (cm^3/g)	Pore size* (μm)	Compressive modulus (kPa)
Salt leached PCL scaffold	0.0961	91.60 ± 0.52	9.56 ± 0.61	421.27 ± 34.18[b]	88.46 ± 15.38
Salt-PEG 200 leached PCL scaffold	0.1012[d]	91.16 ± 1.41[d]	9.18 ± 1.55	378.77 ± 82.13[a, c, d]	28.85 ± 6.80
Salt-PEG 600 leached PCL scaffold	0.0935	91.83 ± 0.61	9.87 ± 0.82	423.07 ± 40.83[b]	42.95 ± 7.85
Salt-PEG 1000 leached PCL scaffold	0.0852[b]	92.56 ± 0.43[b]	10.90 ± 0.68	434.13 ± 36.74[b]	49.98 ± 8.04

3.4.3 Biological Evaluation of PCL Scaffolds

Indirect Cytotoxicity Evaluation

Both mouse calvaria-derived pre-osteoblastic cells (MC3T3-E1) and mouse fibroblasts (L929) were used in this assessment. However, because we were interested in using the obtained constructs as potential bone scaffolds, it was necessary to test the scaffold materials using the L929 cells to comply with the ISO10993-5 standard test method. For both cell types, approximately 40,000 cells/well were seeded in the empty wells of TCPS plates. An indirect cytotoxicity test was the conducted on the salt leached, salt-PEG 200 leached, salt-PEG 600 leached, and salt-PEG 1000 leached PCL scaffolds. Figures 3.8 a) and 3.8 b) show the viability of the cells, which was determined using an MTT assay after the cells had been cultured for 1, 3, or 7 days in extraction media on the experimental scaffolds or in fresh SFM on TCPS, which served as a control. The viability of the cells was reported as a percentage of the viability of the control. The viability ratio of the cells cultured with each extraction medium, as well as of the control cells, was found to be greater than 80%. This result indicates that none of the PCL scaffolds released substances at levels that were harmful to the cells.
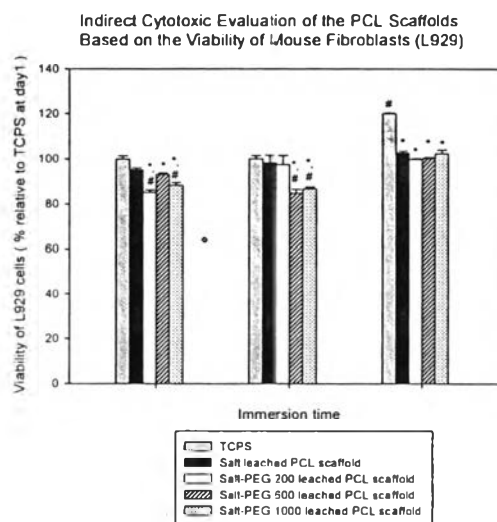
(a)
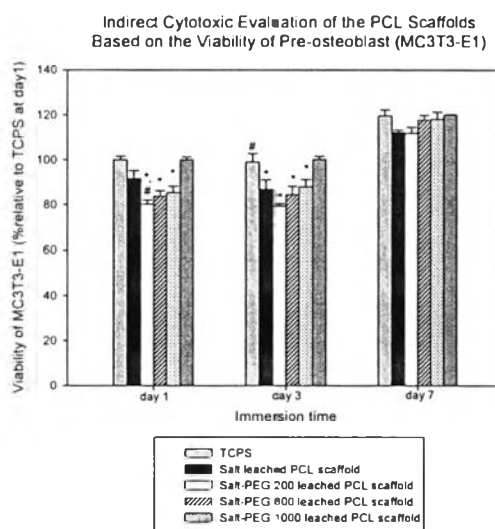
(b)

Figure 3.8 Indirect cytotoxic evaluation of the PCL scaffolds based on the viability of (a) mouse fibroblasts (L929) and (b) pre-osteoblast cells (MC3T3-E1) cultured with the extraction medium from each of these materials, expressed relative to the viability of the cells cultured on the TCPS for 1 day, as a function of the incubation time of the extraction or culture media prior to cell exposure (1, 3, or 7 days). Statistical significance: $*p < 0.05$ compared with the control and $^{\#}p < 0.05$ compared with the salt leached scaffolds at any given time

Cell Attachment and Proliferation

The biocompatibility of each PCL scaffold was evaluated in terms of the scaffold's ability to promote the proliferation of the cells attached to the polymeric surface. Figure 7 shows the proliferation of the MC3T3-E1 cells on the TCPS and the PCL scaffolds after 1-3 days of cell culture, presented in terms of cell viability. The cell viability for each scaffold was quantified using the fluorescent emission intensity from the DNA quantification test. On day1, the viability of the cells on the salt-PEG 1000 leached PCL scaffolds was slightly greater than the viability of the cells cultured on the TCPS, whereas the cells grown on the salt-PEG 200 leached, salt-PEG 600 leached, and salt leached PCL scaffolds were slightly less viable than those cells growing on the TCPS. In contrast, by day 2, the viabilities of the cells on the TCPS and salt leached scaffold were greater than the cell grown on salt-PEG leached constructs. In comparison with TCPS, the cell viability on the salt-PEG 200 leached scaffold was significantly lower. Finally, on day 3, the cell proliferation on the salt-PEG 600 leached and salt-PEG 1000 leached PCL scaffolds was significantly greater than on the TCPS and the salt leached PCL scaffolds.
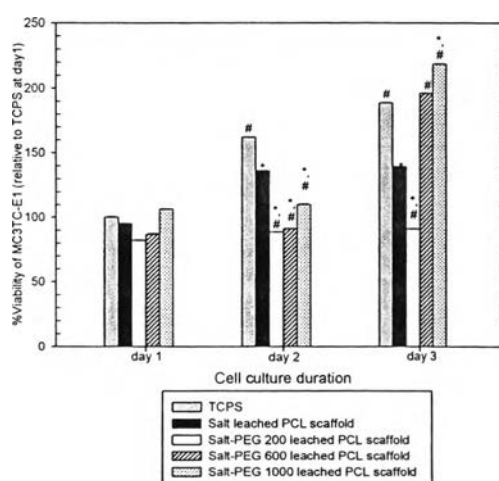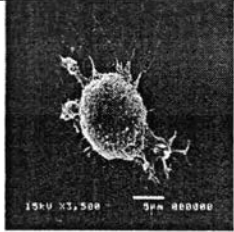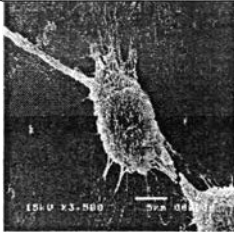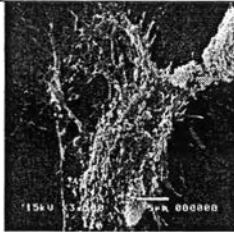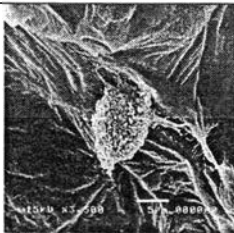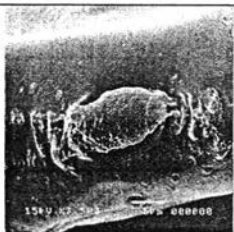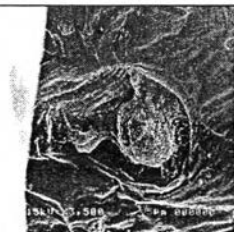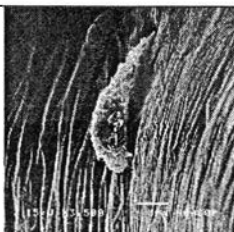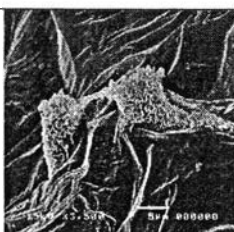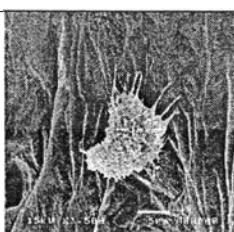

Figure 3.9 Proliferation of the MC3T3-E1 cells cultured on the TCPS surface or seeded on the salt leached and salt-PEG leached PCL scaffolds for 1, 2, or 3 days. Statistical significance: $*p < 0.05$ compared with the control and $^{\#}p < 0.05$ compared with the salt leached PCL scaffolds at any given time point.

Cell Morphology

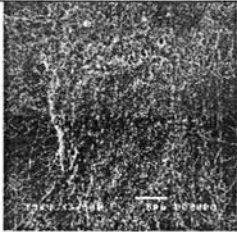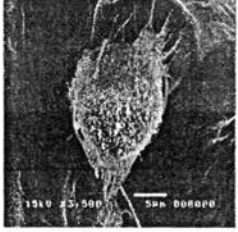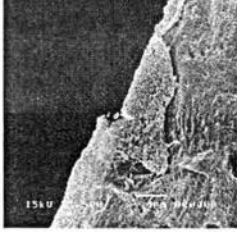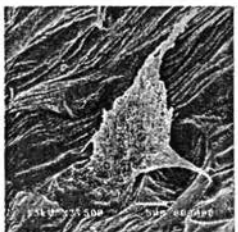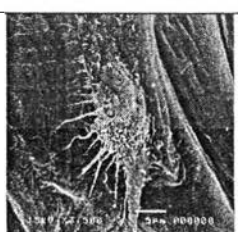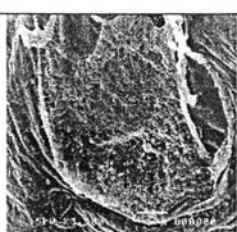Tables 3.3 and 3.4 show selected SEM images (magnification = 3500x; scale bar = 5 μm) of the MC3T3-E1 cells, which were either cultured on glass surfaces or seeded onto salt leached, salt-PEG 200 leached, salt-PEG 600 leached, and salt-PEG 1000 leached PCL scaffolds at different time points. Based on these images, both the cell morphology and the interaction between the cells and the scaffolds can be visualized. At 2 h after cell seeding, the majority of the cells on the glass surface still appeared to have a round morphology. At 4 h after cell seeding, the majority of the cells on the glass surface had begun to extend their cytoplasm, and by 6 h, most of the cells showed evidence of cytoplasm extension. In contrast, for the cells seeded on the various scaffold types, at 2 h after seeding, the majority of the cells appeared round. At 4 h after cell seeding, most of the cells seemed to remain round, but closer examination revealed evidence of filopodia at the cell edges. As a result, by 6 h after seeding, the majority of the cells on the scaffolds were distinctly expanded. Moreover, at 1, 2, and 3 days after seeding, the majority of the cells seeded on all of the scaffold types had expanded over the scaffold surfaces, with the most expansion recorded for the salt-PEG 600 leached and salt-PEG 1000 leached PCL scaffolds.

Table 3.3 Attachment of the MC3T3-E1 cells grown on glass or on the PCL scaffolds for 2, 4, or 6 h. Selected SEM images are presented for the cells on the glass (i.e., the control) and the salt leached, salt-PEG 200 leached, salt-PEG 600 leached, and salt-PEG 1000 leached PCL scaffolds at three different times after cell seeding on the surfaces (magnification = 3500x; scale bar = 5 μm)

Substrate	Culture duration		
	2 h	4 h	6 h
Glass			
Salt leached PCL scaffold			
Salt-PEG 200 leached PCL scaffold			
Salt-PEG 600 leached PCL scaffold			
Salt-PEG 1000 leached PCL scaffold			

Table 3.4 Proliferation of the MC3T3-E1 cells grown on the glass and on the PCL scaffolds for 1, 2, or 3 days. Selected SEM images are presented for the cells on the glass (i.e., the control) and the salt leached, salt-PEG 200 leached, salt-PEG 600 leached, and salt-PEG 1000 leached PCL scaffolds at three different times after cell seeding on the surfaces (magnification = 3500x; scale bar = 5 μm)

Substrate	Culture duration		
	1 day	2 days	3 days
Glass			
Salt leached PCL scaffold			
Salt-PEG 200 leached PCL scaffold			
Salt-PEG 600 leached PCL scaffold			
Salt-PEG 1000 leached PCL scaffold			

ALP Activity

Among the various biological functions of osteoblasts, the secretion of ALP is an important indicator of cellular activity. The ALP activity of the MC3T3-E1 cells cultured on the PCL scaffolds was compared with the activity of the cells maintained on the TCPS (i.e., the control) after 3, 5, and 7 days of culture (Figure 3.10). More specifically, the ALP activity of the MC3T3-E1 cells on the TCPS and the salt leached, salt-PEG 200 leached, salt-PEG 600 leached, and salt-PEG 1000 leached PCL constructs was monitored. For all of the PCL scaffolds investigated, the ALP activity on day 3 was lower than the activity of the cells cultured on the TCPS, whereas the ALP activity on day 5 was very similar for the two surfaces. On day 7, the highest ALP activity of the MC3T3-E1 cells was observed on the salt-PEG 1000 leached scaffolds compared with the TCPS, and the ALP activity of the cells on the salt leached scaffold was lowest, even when compared with the TCPS.
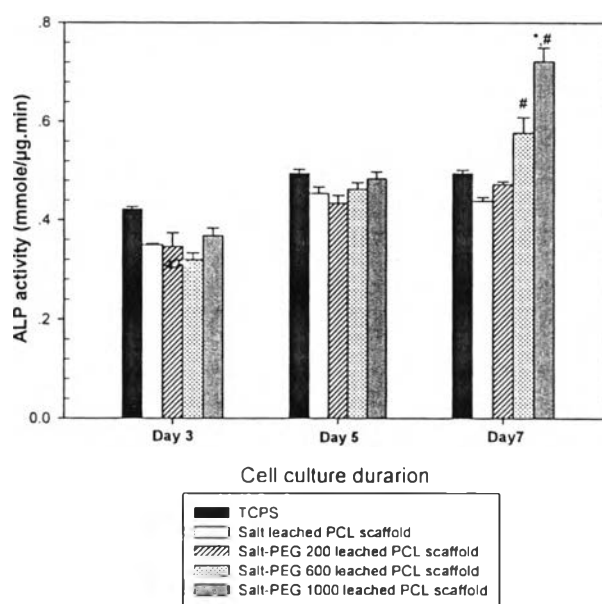
Figure 3.10 ALP activity of the MC3T3-E1 cells cultured on the TCPS surface or seeded on the salt leached and the salt-PEG leached PCL scaffolds for 3, 5, or 7 days. Statistical significance: $*p < 0.05$ compared with the control and $^{#}p < 0.05$ compared with the salt leached PCL scaffolds at any given time point.

Mineralization

Alizarin Red S staining was used to quantify the mineral deposition of the MC3T3-E1 cells cultured on the TCPS and the salt leached, salt-PEG 200 leached, salt-PEG 600 leached, and salt-PEG 1000 leached PCL scaffolds for 14 days. Figure 3.11(a) shows photographic images of the stained specimens. The appearance of red on the stained product indicates the presence of calcium. Quantitative analyses of the results shown in Figure 3.11(b) were performed by eluting the calcium deposits using cetylpyridinium chloride, followed by spectrophotometric analysis at 570 nm. The results revealed that the mineral deposition of the cells cultured on the salt-PEG 600 leached and salt-PEG 1000 leached PCL scaffolds was significantly greater than the mineralization originating from the cells cultured on the salt leached PCL scaffolds and the TCPS.

(a)
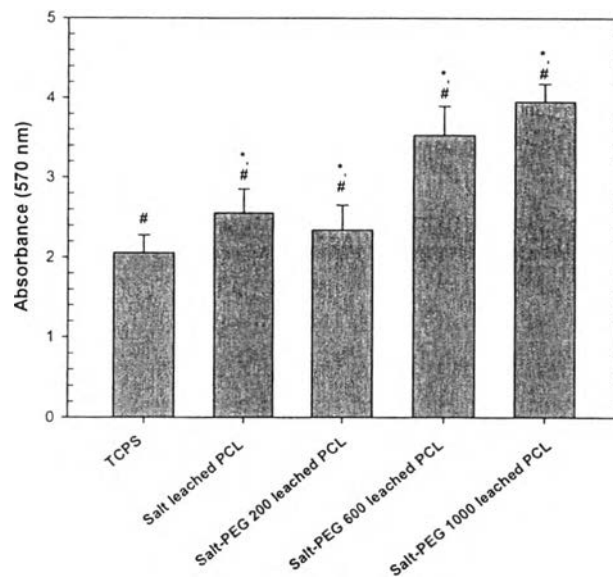
(b)

Figure 3.11 (a) Images of Alizarin Red S staining for the mineral deposition by the MC3T3-E1 cells on day 16 after seeding for the (a) TCPS, (b) salt leached PCL scaffold, (c) salt-PEG 200 leached PCL scaffold, (d) salt-PEG 600 leached PCL scaffold, and 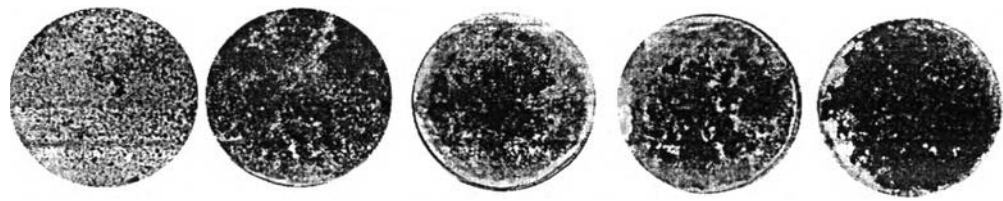(e) salt-PEG 1000 leached PCL scaffold. (b) Quantification of the mineral deposition by the MC3T3-E1 cells based on Alizarin Red S staining. Statistical significance: *$p < 0.05$ compared with the control and #$p < 0.05$ compared with the salt leached PCL scaffolds at any given time point.

3.5 Discussion

The PCL-PEG 1000 blend solution had a higher viscosity than the PCL-PEG 200 and PCL-PEG 600 blend solutions. However, based on Kamide's theory of particle growth during membrane formation,[15] PEG with a molecular weight of 200 or 600 g/mol should exhibit larger diffusion velocities and higher collision frequencies than PEG with a molecular weight of 1,000 g/mol. Hence, in this experimental study, more uniform and interconnected pores were formed by leaching PEG with a molecular weight of 1,000 g/mol, rather than lower molecular-weight PEG. The salt-PEG 600 leached and salt-PEG 1000 leached PCL scaffolds were found to have better hierarchical porous structure and more interconnected pore distributions than the salt-PEG 200 leached PCL constructs. In particular, the pore distribution in the salt-PEG 1000 leached PCL scaffolds was greatest, with more interconnected networks distributed throughout the structures.

The polarities of PCL and PEG are markedly different. Hence, when mixing these materials together, the PEG phase spontaneously dispersed into spherical droplets within the PCL phase, diminishing the surface energy at the PCL-PEG interface.[16] As a result, after the spherical PEG droplets were leached out, interconnected pore networks formed in the salt-PEG leached PCL scaffolds.

Stereomicroscopy, visual slide microscopy and SEM were used to observe the pores, pore distributions, and interconnected pore networks of the scaffolds. The effect of the PEG leaching is illustrated in Figures 3.1-3.5. Figure 3.1 displays the stereomicroscope images of the PCL scaffolds; highly porous structures were obtained for all of the salt and salt-PEG leached PCL scaffolds. Figures 3.2 and 3.3 show the inner morphology of the scaffolds. In particular, the salt-PEG leached PCL scaffolds exhibited high porosity and highly interconnected networks, which was not the case for the salt leached PCL constructs. The pores in the salt-PEG leached scaffolds were interconnected, and the inner surface of the pores appeared relatively coarse. This interconnected pore network is likely capable of facilitating the transport of nutrients and waste, which is beneficial for cell growth and blood vessel invasion. The pore networks and coarse surfaces may also be conducive to coherence and rapid cell propagation.

The interconnectivity and dimensions of the scaffolds' pores affect not only the transport of nutrients into and waste out of the cells but also other scaffold properties. In the current study, scaffold porosity increased with increasing interconnectivity. According to the results presented in Table 3.2, the greatest porosity, pore volume, and pore size values and the highest interconnectivity were observed for the salt-PEG 1000 leached PCL scaffolds, further demonstrating why this construct exhibited the highest water absorption capacity. Such water absorption is an important property of a functional scaffold, facilitating the absorption and retention of wound exudates. Additionally, the passage of exudates through the pore structure may allow particular proteins that are required for bone regeneration to be absorbed into the scaffold surface.[19-21]

For all of the measured distances, the flow resistance was significantly higher for the salt leached PCL scaffolds than for the salt-PEG 200 leached, salt-PEG 600 leached, and salt-PEG 1000 leached PCL. The standard deviation of the flow resistance was higher for the salt-PEG 200 leached and salt-PEG 600 leached PCL scaffolds, indicating the presence of a more irregular structure with a nonuniform distribution of pore interconnectivity in comparison with the salt-PEG 1000 leached PCL constructs. Moreover, the higher percentage of closed pores may account for the increased flow resistance observed for all of the salt leached PCL scaffolds.

The higher porosity (92.6% in comparison with 91.6%) of the scaffolds decreased the compressive modulus from 88 to 49 kPa. Porosity is an important scaffold parameter that plays a significant role in encouraging cell proliferation and growth. Higher porosities provide cells with spacious surroundings for propagation. However, if the porosity is too high,[22] the scaffolds may not be able to maintain enough mechanical rigidity.[23] For example, although increased porosity facilitates bone ingrowth, another result is a reduction in the scaffold's mechanical properties, as porosity is central to structural integrity.[24]

The biocompatibility of these PCL scaffolds, intended for use as bone scaffolds, was assessed by an indirect cytotoxicity evaluation of mouse fibroblasts (L929) and mouse calvaria-derived pre-osteoblastic cells (MC3T3-E1), based on an initial seeding density of 40,000 cells/well. Although we were interested in using the obtained constructs as potential bone scaffolds, it was also necessary to test the

materials using the L929 cells to comply with the ISO10993-5 standard test method. The viability ratio of the cells cultured in each extraction medium and on the TCPS, which served as a control, was found to be greater than 80%. These results suggest that none of the PCL scaffold types investigated released substances at levels that could be harmful to either cell type. Similar to our results, Jie et al.[25] showed that the cytotoxicity of poly(D,L-lactide)/nano-hydroxyapatite composites was 79.6-82.6% and found that the cytotoxicity of these scaffolds was grade I according to ISO10993-1, meaning that these materials exhibited high cytocompatibility.

In comparison with the cells grown on the TCPS, the viability of the cells on the salt-PEG 200 leached, salt-PEG 600 leached, and salt leached PCL scaffolds was slightly lower on day 1. However, by day 3, the proliferation of the cells on the salt-PEG 600 leached and salt-PEG 1000 leached PCL scaffolds was significantly greater than on the control surface. Reduced cell viability was also observed during the attachment period for the various types of scaffolds in comparison with the TCPS. In contrast, the greater number of cells observed during the proliferation period on the PCL scaffolds could be the result of the high porosity and highly interconnected pore networks of the PCL scaffolds, allowing the cells to penetrate into the scaffolds. As a result, higher porosity did not affect cell attachment but resulted in increased cell proliferation due to the pores' facilitation of the transport of oxygen and nutrients.[24,26]

The ALP activity of the MC3T3-E1 cells was measured to compare the effects of the different scaffold types on osteoblastic differentiation over 3, 5, or 7 days of culture on the PCL scaffolds. As shown in Figure 4.1.10, the ALP activity of the cells cultured on the salt-PEG 1000 leached PCL scaffolds was significantly higher than the activity of the cells grown on the TCPS on day 7. When the culture was maintained for up to 14 days, significantly greater amounts of calcium were deposited on the salt-PEG 1000 leached PCL scaffolds than on the TCPS surface and the salt leached PCL scaffolds, as determined by Alizarin Red S staining and the quantification of calcium deposition. Based on all of the results presented here, the biocompatibility of the salt-PEG 1000 leached PCL scaffolds may be the result of the high porosity and highly interconnected network of the constructs, permitting cell intrusion and permeation.

3.6 Conclusion

In sum, 3D PCL scaffolds with highly porous and interconnected networks can be prepared using our modified solvent casting, particulate leaching, and polymer leaching techniques, which implement sodium chloride and PEG as porogens. SEM, visual slide microscopy and optical microscopy confirmed that the scaffolds fabricated using this method exhibit highly interconnected pore networks, equally distributed pores, and a relatively uniform pore size of 378-435 μm. The greatest porosity, pore volume, and pore size values and the highest interconnectivity were observed for the salt-PEG 1000 leached PCL scaffolds, further leading to the highest water absorption capacity of the materials tested.

The potential for the use of these constructs in bone tissue engineering was evaluated in vitro using mouse calvaria-derived pre-osteoblastic cells (MC3T3-E1). An indirect cytotoxicity evaluation revealed that the scaffolds fabricated using our method released no substances at levels that were harmful to the cells. Moreover, SEM demonstrated that the majority of the cells seeded on the scaffold surfaces had expanded over the scaffold surface after 3 days, with the most expansion observed on the scaffolds generated by our method. The cells cultured on these new PCL scaffolds also yielded the highest mineral deposition values. Taken together, all of our results indicate the potential use of these constructs as bone scaffolds.

3.7 Acknowledgements

3.8 References

[1]   Hyun JC, Tae GP. Surface engineered and drug releasing pre-fabricated scaffolds for tissue engineering. Adv Drug Deliv Rev 2007; 59: 249-262.

[2]   Woesz A, Rapid Prototyping to Produce POROUS SCAFFOLDSWITH CONTROLLED ARCHITECTURE for Possible use in Bone Tissue Engineering. Virtual Prototyping & Bio Manufacturing in Medical Applications 2008; 9: 171-205.

[3]   Sinha VR, Bansal K, Kaushik R, Kumiria R, Trehan A. Poly-ε-caprolactone microspheres and nanospheres:an overview. Int J of Pharm 2004; 278(1): 1-23.

[4]   Nam YS, Park TG. Porous Biodegradatle Polymeric Scaffolds by Thermally Induced Phase Separation. Biomed Mater Res 1999; 47 (1): 7-17.

[5]   Hutmacher DW. Scaffolds in tissue engineering bone and cartilage. Biomater Sci Polym Ed 2001; 12 (1): 107-24.

[6]   Lee JH, Park TG, Park HS, Lee DS, Lee YK, Yoon SC, Nam J. Thermal and mechanical characteristics of poly(l-lactic acid) nanocomposite scaffold. Biomater 2003; 24: 2773-2778.

[7]   Carletti E, Motta A, Migliaresi C. Scaffolds for Tissue Engineering and 3D Cell Culture. Methods in Mol Biol, 695, 17-39.

[8]   Kim HJ, Kim UJ, Leisk GG, Bayan C, Georgakoudi I, Kaplan DL. Bone regeneration on macroporous aqueous-derived silk 3-D scaffolds. Macromol Biosci 2007; 7: 643-655.

[9]   Pattison MA, Wurster S, Webster TJ, Haberstroh KM. Three-dimensional, nano-structured PLGAscaffolds for bladder tissue replacement applications. Biomater 2005; 25: 2491-2500 .

[10]   Yoon JJ, Song SH, Lee SS, Park TG. Immobilization of cell adhesive RGDpeptide onto the surface of highly porous biodegradable polymer scaffolds fabricated by a gas foaming/salt leaching method. Biomater 2004; 25: 5613-5620.

[11]   Shin M, Abukawa H, Troulis MJ, Vacanti JP. Development of abiodegradable scaffold with interconnected pores by heat fusion and its application to bone tissue engineering. Biomed Mater Res A. 2008; 84A: 702-709.

[12]   Sokolsky-Papkov M, Agashi K, Olaye A, Shakesheff K, Domb AJ. Polymer carriers for drug delivery in tissue engineering. Adv Drug Deliv Rev 2007, 59, 187-206.

[13]   Cao Y, Croll T, Lees JG, Tuch BE, Cooper-White JJ. Scaffolds, stem cells, and tissue engineering: A potent combination. Aust J Chem 2005; 58 (10): 691-703.

[14]   Ekaputra AK, Prestwich GD, Cool SM, Hutmacher DW. Combining Electrospun Scaffolds with Electrosprayed Hydrogels Leads to Three-Dimensional Cellularization of Hybrid Constructs. Biomacromol 2008; 9: 2097-2103.

[15]   Lin WJ, Lu CK. Characterization and permeation of microporous poly(ε-caprolactone) films. J Membr Sci 2002; 198: 109-118.

[16]   Lin WJ, Lee HG. D esign of a microporous controlled delivery system for theophylline tablets. J controlled Release 2003; 89: 179-187.

[17]   Kesting RE. Synthetic Polymeric Membranes: A Structural Perspective John Wiley & Sons 1985; 348 pp.

[18]   Harris JM. Poly(ethylene Glycol) Chemistry : Biotechnical and Biomedical Applications 1992; 408 p.

[19]   Yang G, Zhang HF. Role of polyethylene glycol in formation and structure of regenerated cellulose microporous membrane. J Membr Sci 1999; 161: 31.

[20]   Chuenjitkuntawown B, Inrung W, Damrongsri D, Mekaapiruk K, Supaphol P, Pavasant P. Polycaprolactone/Hydroxyapatite composite scaffolds: Preparation, characterization, and in vitro and in vivo biological responses of human primary bone cells. J Biomed Mater Res Part A 2009; 241-251.

[21]   Hariraksapitak P, Suwantong O, Pavasant P, Supaphol P. Effectual drug-releasing porous scaffolds from 1,6-diisocyanatohexane-extended poly(1,4-butylene succinate) for bone tissue regeneration. Polym 2008; 49: 2678-2685.

[22]   Mikos AG, Sarakinos G, Lyman MD, Ingber DE, Vacanti, JP, Langer RS. Prevascularization of porous biodegradable polymers. Biotechnol Bioeng 1993; 42: 716-723.

[23]   Yang Q, Chen L, Shen XY, Tan ZQ. Preparation of Polycaprolactone Tissue Engineering Scaffolds by Improved Solvent Casting/Particulate Leaching Method. J Macromol Sci B: Phys 2006; 45: 1171-1181.

[24] Karageorgiou V, Kaplan D. Porosity of 3D biomaterial scaffolds and osteogenesis. Biomater 2005; 26: 5474-5491.

[25] Ren J, Zhao P, Ren T, Gu S, Pan K. Poly (D,L-lactide)/nanohydroxyapatite composite scaffolds for bone tissue engineering and biocompatibility evaluation. J Mater Sci: Mater Med 2008; 19: 1075-1082.

[26] Takahashi Y, Tabata YJ. Effect of the fiber diameter and porosity of non-woven PET fabrics on the osteogenic differentiation of mesenchymal stem cells. Biomater Sci Polym Ed 2004; 15(1): 41-57.

[27] Lee H, Park TG. Design Principles in Biomaterials and scaffold; 33: 580-593.

[28] Desmet T, Morent R, Geyter ND, Leys C, Schacht E, Dubruel P. Nonthermal plasma technology as a versatile strategy for polymeric biomaterials surface modification: A review. Biomacromol 2009; 10(9): 2351-2378.

[29] Lee HJ, Ahn SH, Kim GH. Three-Dimensional Collagen/Alginate Hybrid Scaffolds Functionalized with a Drug Delivery System (DDS) for Bone Tissue Regeneration. Chem Mater 2011; 10.

[30] Draghi L, Resta S, Pirozzolo MG, Tanzi MC. Microspheres leaching for scaffold porosity control. J Mater Sc: Mater Med 2005; 16: 1093 – 1097.

[31] Stamatialis DF, Papenburg BJ, Girones M, Saiful S, Bettahalli SNM, Schmitmeier S, Wessling M. Medical applications of membranes: Drug delivery, artificial organs and tissue engineering. J Membr Sci 2008; 308: 1-34.

[32] Lee CT, Huang CP, Lee YD. Biomimetic Porous Scaffolds Made from Poly(L-lactide)-g-chondroitin Sulfate Blend with Poly(L-lactide) for Cartilage Tissue Engineering. Biomacromol 2006; 7: 2200-2209.

[33] Lim YM, Gwon HJ, Shin J, Jeun JP, Nho YC. Preparation of porous poly(e-caprolactone) scaffolds by gas foaming process and in vitro/in vivo degradation behavior using g-ray irradiation. J Ind Eng Chem 2008, 14, 436-441.

[34] Sarazin P, Roy X, Favis BD. Controlled preparation and properties of porous poly(l-lactide) obtained from a co-continuous blend of two biodegradable polymers. Biomater 2004; 25: 5965-5978.

[35] Dorati R, Colonna C, Genta I, Modena T, Conti B. Effect of porogen on the physico-chemical properties and degradation performance of PLGA scaffolds. Polym Degrad Stab 2010; 95: 694-701.

[36]   Rezwan K, Chen QZ, Blaker JJ, Boccacini AR. Biodegradable and bioactive porous polymer/inorganic composite scaffolds for bone tissue engineering Biomater 2006; 27: 3413-3431.

[37]   Wutticharoenmongkol P, Pavasant P, Supaphol P. Osteoblastic Phenotype Expression of MC3T3-E1 Cultured on Electrospun Polycaprolactone Fiber Mats Filled with Hydroxyapatite Nanoparticles. Biomacromol 2007; 8: 2602-2610.

[38]   Lee YH, Lee JH, An IG, Kim C, Lee DS, Lee YK, Nam JD. Electrospun dual-porosity structure and biodegradation morphology of Montmorillonite reinforced PLLA nanocomposite scaffolds. Biomater 2005; 26: 3165-3172.

[39]   Shum AWT, Li J, Mak AFT. Fabrication and structural characterization of porous biodegradable poly(DL-lactic-co-glycolic acid) scaffolds with controlled range of pore sizes. Polym Degrad Stab 2005; 87: 487-493.

[40]   Sombatmankhong K, Sanchavanakit N, Pavasant P, Supaphol P. Bone scaffolds from electrospun fiber mats of poly(3-hydroxybutyrate), poly(3-hydroxybutyrate-co-3-hydroxyvalerate) and their blend. Polym 2007; 48: 1419-1427.

[41]   Sangsanoh P, Waleetorncheepsawat S, Suwantong O, Wuttcharoenmongkol P, Weeranantanapan O, Chuenjitbuntaworn B, Cheepsunthorn P, Pavasant P, Supaphol P. In Vitro Biocompatibility of Schwann Cells on Surfaces of Biocompatible Polymeric Electrospun Fibrous and Solution-Cast Film Scaffolds. Biomacromol 2007; 8: 1587-1594.

[42]   Chuenjitbuntaworn B, Supaphol P, Pavasant P, Damrongsri D. Electrospun poly(L-lactic acid)/hydroxyapatite composite fibrous scaffolds for bone tissue engineering. Polym Int 2010; 59: 227-235.

[43]   Wutticharoenmongkol P, Sanchavanakit N, Pavasant P, Supaphol P. Preparation and Characterization of Novel Bone Scaffolds Based on Electrospun Polycaprolactone Fibers Filled with Nanoparticles. J Nanosci and Nanotechnol 2006; 6: 514-522.

[44]   Yang Q, Chen L, Shen X, Tan Z. J Macromol Sci B: Phys 2006; 45: 1171-1181 .